European Journal of Chemistry

View Journal Online
View Article Online

Alendronate functionalized PLGA based nanoparticles for the effective treatment of osteoporosis-Formulation to *in-vitro* release kinetic studies

Sandhya Pathak *, Sandeep Shukla, Bharat Patel, Satyendra Kumar Tripathi and Archna Pandey

Department of Chemistry, Dr. Harisingh Gour Vishwavidyalaya, Sagar, 470003, Madhya Pradesh, India

* *Corresponding author at: Department of Chemistry, Dr. Harisingh Gour Vishwavidyalaya, Sagar, 470003, Madhya Pradesh, India.*
e-mail: sandhyapathak935@gmail.com (S. Pathak).

RESEARCH ARTICLE

10.5155/eurjchem.13.4.407-414.2246

Received: 07 March 2022
Received in revised form: 19 September 2022
Accepted: 24 September 2022
Published online: 31 December 2022
Printed: 31 December 2022

KEYWORDS

Alendronate
Osteoporosis
Bisphosphonate
Release kinetics
Nanoprecipitation
Bone mineral density

ABSTRACT

Osteoporosis is a bone disease caused due to the reducing bone mineral density. Porous and more fragile bones increase the risk of fractures. Hip, spine, shoulder, and wrist bones are commonly affected by osteoporosis. Low bone density is a leading cause of osteoporosis. The most efficient prescribed drugs for the treatment of osteoporosis are bisphosphonates drugs. Alendronate was the first FDA approved bisphosphonate drug for the treatment of osteoporosis. Osteoclast cells are the primary targeting site for alendronate, responsible for bone resorption. A biopharmaceutical classification system class III bisphosphonate acts as a potent, efficient, and bone resorption inhibitor drug. In the present study, alendronate functionalized PLGA based nanoparticles were developed by a solvent diffusion method and optimized for different process variables. The formulated nanoparticles were characterized for surface morphology, particle size distribution, surface charge and drug-polymer compatibility. The scanning electron microscopy and transmission electron microscopy results showed nanoparticle size in the range below 200 nm. The average particle size and zeta potential of the formulated nanoparticles were found to be 175.3 nm and -13.98 mV, respectively. The highest encapsulation efficiency was 65.23%. The release profile was dissolution medium dependent and followed by the Higuchi model of release kinetics.

Cite this: *Eur. J. Chem.* **2022**, *13(4)*, 407-414 **Journal website**: www.eurjchem.com

1. Introduction

Decreasing bone mineral density (BMD) is the leading cause of osteoporosis. Spinal and hip fractures are the most dangerous consequences of osteoporosis. Generally, it is seen in old age, but women face this problem after menopause called postmenopausal osteoporosis (PMO) [1,2]. The most efficient, FDA (The Food and Drug Administration, USA) approved drugs for treating osteoporosis are bisphosphonates. Bisphosphonate efficacy has been well established in large clinical trials. FDA firstly approved alendronate in the US in 1995. Alendronate targets osteoclast cells and inhibits bone resorption, so it is recommended as a potent drug for the treatment of osteoporosis in medical trials. Since then, newer molecules of bisphosphonates have been introduced to improve previous compliance, *i.e.*, ibandronate, risedronate, pamidronate, *etc.* [3,4]. Alendronate is highly efficient but presents low absorption after oral administration; burst release occurs due to high water solubility (Figure 1). Low systemic bioavailability and burst release of the drug inside the body are the main challenges in alendronate drug delivery systems. Drug nanocarriers help reduce toxicity, improve solubility and bioavailability, enhance release, and provide better drug formulation opportunities [5-7].

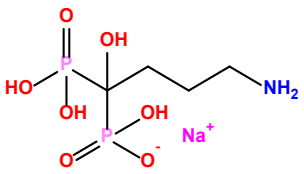

Figure 1. Chemical structure of alendronate sodium.

Low bioavailability, long-term treatment, and adverse effects on body organs are significant problems in the clinical development of several drugs, so research is currently going on to solve these problems. Recently, nanocarrier-based drug delivery systems like polymeric nanoparticles (NPs), solid lipid NPs (SLNs), nanoemulsions, liposomes, nanosuspension and micelles have been presenting novel drug delivery systems for improving the drug solubility and enhancing the oral bioavailability of drugs. Today, polymeric nanoparticles have been proven to be efficient drug nanocarriers [8-11]. Polymeric nanoparticles have long played an important role in drug delivery due to their biocompatibility and ability to encapsulate drug molecules that are otherwise too hydrophobic for effective pharmacological formulation. These drug-loaded polymeric matrix particles are usually on the order of 10-1000 nm, and

https://dx.doi.org/10.5155/eurjchem.13.4.407-414.2246

since they are biodegradable, the drug release rate can be tuned through the polymer composition [12-14].

Synthetic biodegradable polymers such as polylactide (PLA) and copolymer poly(lactide-co-glycolide) (PLGA) have been extensively used for the synthesis of nanoparticles because of their biocompatibility, nontoxicity, and tunable degradation rates. It is possible to achieve different drug release profiles by modifying the molecular weight, the copolymer ratio, the particle size, and the process variables. The FDA has approved it for several biomedical applications due to the specific properties of PLGA, such as swelling, the potential for molecular interaction, and the controllable degradation period (approximately 1-6 months), which makes it suitable for the design of controlled delivery systems [15,16].

In the present study, alendronate loaded PLGA NPs were developed to maintain sustained drug release and reduce burst release from drug NPs. The nanoparticles were prepared by the modified nanoprecipitation method and characterized with the help of dynamic light scattering (DLS), scanning electron microscopy (SEM), and transmission electron microscopy (TEM) and atomic force microscopy (AFM). The results revealed that the nanoprecipitation method is suitable for preparing nanoparticle formulation. The drug entrapment efficiency of the particles varied depending on the drug-polymer ratio. The study of drug release kinetics of formulated drug-loaded NPs was performed using different mathematical models [17-19].

2. Experimental

2.1. Materials

Alendronate-sodium (Mw: 249.09 g/mol) was purchased from Sigma-Aldrich (Mumbai, India). Poly(lactide-co-glycolide), PLGA (50:50), polyvinyl alcohol (PVA), and acetone were purchased from Sigma Aldrich (India). Dialysis membrane of the diameter of 16 mm (M.w. cut-off: 12000 Da and flat with 25 mm) was purchased from Himedia (India). All other chemicals and reagents were of analytical grade.

2.2. Formulation of alendronate loaded PLGA NPs

Alendronate-loaded PLGA NPs were prepared using the solvent diffusion method (nanoprecipitation) [20-22]. Different amounts (10, 20, and 40 mg) of polymer (PLGA) were dissolved in 10 mL of organic solvent (acetone) and stirred well up to complete dissolution to form the organic phase. The aqueous phase contained a surfactant (PVA) with water. Both phases were sonicated for 40 seconds under a bath sonicator. The organic phase was added dropwise to the aqueous phase, containing 0.5% (w/v) PVA and 10 mg of alendronate drug. Different drug to polymer ratios (1:1, 1:2, and 1:4) were taken for optimization. The suspension obtained was stirred on a magnetic stirrer for 3-4 hours. An excess amount of organic solvent was evaporated by rotavapor. The formulated polymeric NPs were evaluated for average particle size, polydispersity index (PDI), and zeta potential (surface charge) by using the DLS instrument. The dialysis membrane method was used for release kinetic studies [23,24].

The obtained nanosuspension was centrifuged at 14000 rpm for 30 min by an ultracentrifuge and entrapment efficiency was determined by UV-Visible detection of supernatant. Nanoparticle pellets were washed with distilled water twice and the remaining suspended NPs were lyophilized by instrument (LAMBCONCO, GNCIIM) for future solid-state characterization such as Fourier transform infrared spectroscopy (FTIR) and differential scanning calorimetry (DSC) [25-27].

2.3. Entrapment efficiency of alendronate loaded PLGA NPs

The entrapment efficiency (EE) of alendronate loaded PLGA NPs was determined by the indirect method. Alendronate does not show absorbance in the ultraviolet (UV) region, so complex formation is required for the spectrophotometric study. The amount of unentrapped drug in the supernatant was determined using the method developed by Ostovic *et al.* and used by Cohen-Sela *et al.* [28,29]. EE% was determined at 240 nm wavelength following the addition of copper(II) reagent (5 mM copper sulfate in 1.5×10^{-3} M HNO_3) by complexation between alendronate and copper ions. The amount of encapsulated drug was obtained using a UV-Vis spectrophotometer after proper dilution. The experiment was carried out in triplicate and the average value was considered for the final calculation. The following formula was used to calculate the entrapment efficiency (% EE);

$$\text{Entrapment efficiency (\%)} = (\text{Weight of drug in nanoparticles})/(\text{Weight of drug added initially})\times100 \quad (1)$$

where drug in particles = Total amount of drug initially added - Amount of drug in the supernatant.

2.4. Characterization

2.4.1. Particle size and surface charge determination

Photon correlation spectroscopy (PCS) based studies were performed for evaluation of poly dispersity index (PDI), average particle size, and zeta Potential (ZP) of formulated alendronate-loaded PLGA NPs through dynamic light scattering analysis with Malvern Zeta sizer Nano S (Malvern, UK).

2.4.2. Morphological study

Scanning electron microscope (SEM) technique was used to study the surface morphology of the best formulation. A single drop of sample was poured into a circular aluminium plate and dried in a vacuum oven until a dry film was created, then it was observed under the SEM instrument (NOVA NANO FESEM 450). Transmission electron microscope (TEM) is another technique used for the confirmation of the surface morphology of formulated NPs. A small amount of NPs suspension was dispersed into distilled water. A single drop of nanosuspension was placed on a paraffin sheet, and a carbon-coated grid was placed on the sample and left for some time to allow the alendronate PLGA-NPs to stick on the carbon substrate. The extra suspension was removed by adsorbing with a piece of filter paper. Then the grid was placed on a drop of phosphotungstate for 10 seconds and the sample was air dried. The prepared sample was examined by TEM instrument (TECNA) and AFM (INNOVA, ICON Analytical Equipment, Bruker).

2.4.3. Fourier transform infrared (FTIR) studies

The interaction between drug and polymer was identified from the Fourier-transform infrared spectroscopy (FTIR) (Bruker Tensor37). The FTIR spectrum of pure drug alendronate and alendronate-loaded PLGA NPs were obtained. The samples were prepared by grinding with anhydrous KBr powder and compressed into pellets. The FTIR spectra of drug and drug-loaded NPs were measured over the range of 4000-400 cm^{-1}.

2.4.4. Drug-excipient compatibility studies by differential scanning calorimeter

Thermal analysis of any endothermic processes (Melting, solid-solid phase transitions and chemical degradation) and

exothermic processes (Crystallization and oxidative decomposition) is done by a common technique differential scanning calorimeter (DSC). Generally, it is used in preformulation studies of any drug; it confirms the existence of probable drug-excipient or excipient-excipient interactions in any new formulation. Thermograms of pure drug (Alendronate) and alendronate loaded PLGA NPs were obtained by using DSC instrument (NETZSCH, STA 449 F1 Jupiter). The samples were taken directly into a DSC aluminium pan and scanned in the temperature range of 25-300 ° C in a dry nitrogen atmosphere. A heating rate of 10 °C/min was used, and thermograms were obtained and confirmed the interaction between the drug and the excipient.

2.5. Drug release kinetic studies

The dialysis bag approach was used to investigate the drug release kinetics of formulated NPs. In phosphate buffer saline (PBS) pH = 6.8, temperature at 37±2 °C, a membrane with a pore size of 2.4 nm and a molecular weight cut-off between 12,000 and 14,000 was utilized. The drug-loaded NPs were inserted into a dialysis membrane, knotted at both ends, and placed in a 100 mL diffusion medium beaker (PBS of pH = 6.8). The magnetic stirrer was used to keep the temperature and speed at 37±2 °C and 100 rpm, respectively. To maintain the sink condition, the aliquot samples were taken at predefined intervals and replaced with fresh buffer in the same volume. For alendronate, the amount of medication released was measured spectrophotometrically at 240 nm (complex formation method). The amount of drug released was used to compute the cumulative percentage release. Some mathematical kinetic models (Zero order, first order, Higuch's model and Korsmeyer-Peppas model) were used to determine release kinetics. The linear curve generated by regression analysis of the plots was used to calculate the R^2 and k values [30-33]. *In-vitro* drug release studies were performed using the dialysis bag method for different mathematical kinetic models. For the kinetic study of formulated drug NPs, the plots were made in the following way: (i) Zero-order kinetic model (% Cumulative drug release *vs* time), (ii) First-order kinetic model (Log % Cumulative drug remaining *vs* time), (iii) Higuchi model cumulative (% Drug release *vs* square root of time) and (iv) Korsmeyer-Peppas model (Log % Cumulative drug release *vs* Log time).

3. Results and discussion

3.1. Experimental design

Alendronate-loaded PLGA NPs were generated in this investigation utilizing the nanoprecipitation process, as illustrated in Figure 2, which involved the use of a polymer (PLGA) and a surfactant (PVA). To create the optimum formulation, different drug-to-polymer ratios were used, such as 1:1, 1:2, and 1:4. The best result of the 1:4 ratios of medication and polymer was disclosed by the findings of particle size analysis and potential investigation. The entrapment efficiency has changed significantly as the concentration of PVA has changed.

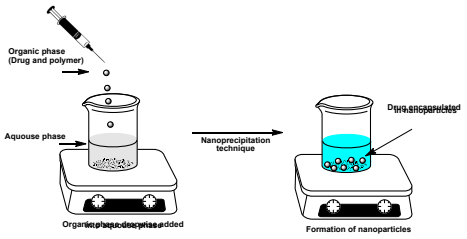

Figure 2. Diagrammatic presentation of the nanoprecipitation method.

3.2. Optimization

Using the solvent diffusion approach, a variety of process factors were evaluated to determine appropriate preparation conditions, including sonication time, polymer concentration, and surfactant concentration, among others. In each experiment, only one variable was changed.

3.2.1. Sonication time effect

The sonication period was changed between 10 and 40 minutes to improve the influence of the sonication time on the size and shape of the nanoparticles (Figure 3). According to the TEM picture of the nanoparticles with the smallest size in this series of formulations, the nanoparticles were spherical in shape. On the basis of the findings, it can be concluded that increasing the duration of sonication causes the size of the nanoparticles to drop from 320 to 185 nm.

3.2.2. Effect of polymer concentration

Polymer concentration was varied in the range of 10 to 40 mg in the organic phase, and the impact of the initial quantity of polymer on particle size and shape was studied at the same time as preserving all process variables under standard conditions (Figure 3). The increasing the polymer concentration starting from 10 to 40 mg in the organic phase led to an increase in nanoparticle size from 210 to 280 nm. The size of the nanoparticles increased with increasing polymer concentration in the organic phase because the viscous nature of the dispersed phase increased. Consequently, the organic phase into the aqueous phase diffusion reduced and resulted in the bigger size particle formation during the diffusion process.

3.2.3. Effect of surfactant concentration

The surfactant (PVA) concentration effect on particle size and shape was investigated in a series of formulation prepared using an aqueous phase containing PVA of different concentrations (0.25 to 1.00%) (w/v), while keeping all other parameters constant. The results indicated two findings (i) When the PVA concentration increased, the size of the nanoparticles first decreased (320 to 230 nm) and (ii) Gradually, the size of the nanoparticles increased from 230 to 380 nm (Figure 3). The optimized formulation of alendronate-loaded PLGA NPs was selected based on the minimum particle size and maximum entrapment efficiency values and applied for further studies.

3.3. Characterization

The FTIR spectra of pure drug alendronate and drug-loaded NPs were obtained by using FTIR to characterize the chemical structure of biopolymer and nanoparticle (Figure 4). The main characteristic peaks of alendronate-sodium show at 1186 and 1064 cm^{-1} in the region 1200-900 cm^{-1} correspond to C=O and P=O stretching modes, respectively. The characteristic peak of phosphate group of alendronate is obtained at 1551 cm^{-1}. All characteristic peaks are also present in the FTIR spectrum of alendronate-loaded PLGA NPs with minor shifting of the peaks. The absence of the characteristic peak of the phosphate group of the drug alendronate at 1551 cm^{-1} shows that the drug molecules were entrapped in polymeric nanoparticles.

3.4. Nanoparticle size of the optimized formulation

The nanoprecipitation method was used to prepare the alendronate-loaded PLGA NPs in the desired range and it was considered an efficient nanocarrier for drug encapsulation.

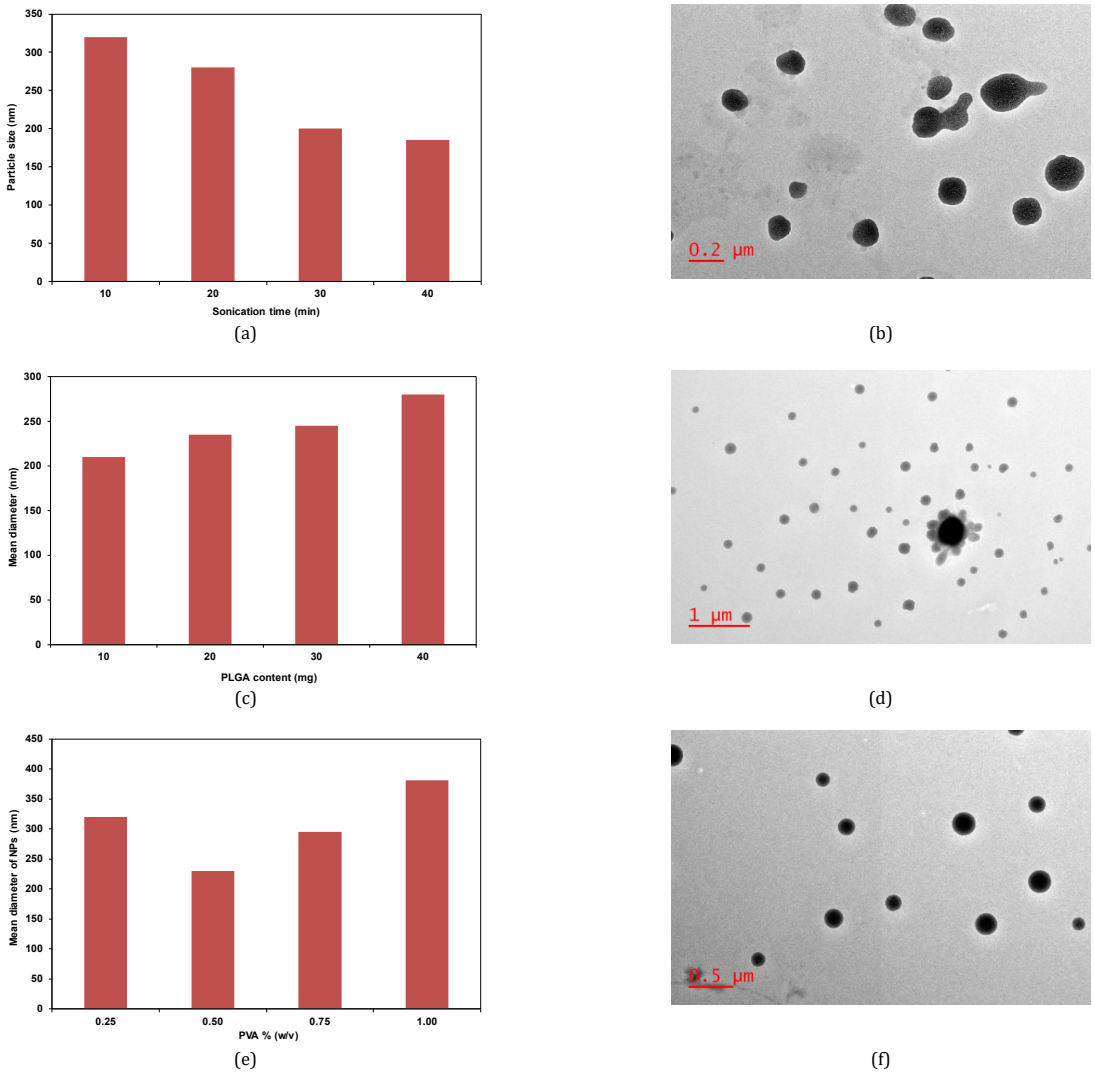

Figure 3. (a) Sonication time effect on particle size, (b) TEM image of optimized formulation after 40 minutes sonication with least mean particle size, (c) Polymer (PLGA) content effect in organic phase on the size of nanoparticles, (d) TEM image of the best formulation prepared with 40 mg PLGA in organic phase, (e) Effect of surfactant (PVA) content on the size of nanoparticles and (f) TEM image of the nanoparticles prepared with 0.5 % w/v PVA in aqueous phase.

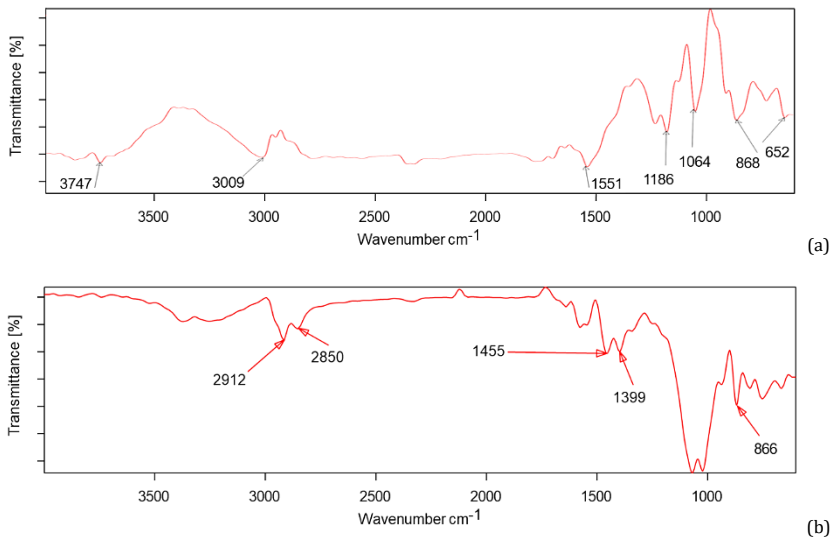

Figure 4. The FTIR spectrum of (a) pure drug alendronate and (b) alendronate-loaded PLGA NP.

Table 1. Comparison b/w Alendronate loaded Chitosan and PLGA nanoparticles.

Characterization	Alendronate loaded chitosan NPs	Alendronate loaded PLGA NPs
Average particle size (nm)	214.6	175.3
Polydispersity index	0.156	0.143
Zeta potential (mV)	+24.1	-13.98
Entrapment efficiency (%)	66.82	65.23

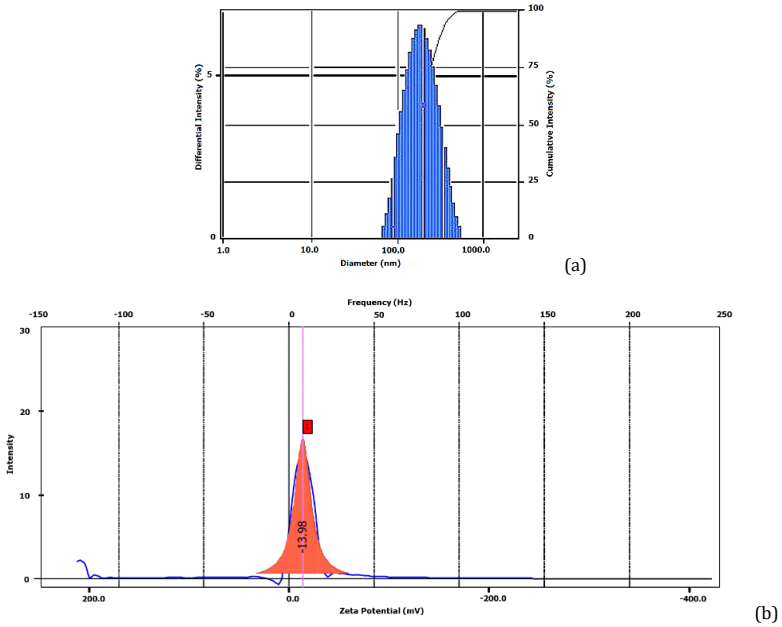

Figure 5. (a) Average particle size of alendronate PLGA NPs and (b) Zeta potential of alendronate PLGA NPs (Mean±SD, n = 3).

This method is widely used for nanoformulation as a result of its simple methodology, nontoxic nature, and cost-effectiveness. The prepared alendronate loaded PLGA NPs were found in the nano range. The results of DLS studies for average particle size, distribution and zeta potential are shown below in Figure 5, and their spherical shapes were confirmed by using TEM, SEM and AFM in Figure 6.

The optimized formulation showed the average particle size (175.3 nm), entrapment efficiency (65.23%) and polydispersity index (PDI) was 0.143. The zeta potential of the optimized formulation was found to be -13.98 mV. The drug and polymer ratio of the optimized formulation was 1:4, which shows the average particle size in the range below 200 nm.

In our previous work, we also prepared alendronate-loaded chitosan NP [34]. The results of average particle size, PDI, zeta potential, and % entrapment efficiency are compared in the following Table 1.

In the above results, the average size of drug-loaded PLGA NPs is smaller than that of chitosan NPs because agglomeration in chitosan NPs via the ionotropic gelation method increased the size of the NPs. The polydispersity index is used to determine the degree of polymerization. Polydispersity index values of 0.2 and below are most commonly acceptable in practice for polymer-based NPs. PDI value for PLGA and chitosan NPs is in the acceptable range. The zeta potential value represents the surface charge of NPs. PLGA being a negatively charged polymer imparts anionic nature to nanoparticles where Zeta potential value was found as -13.98 mV, while in chitosan NPs, the value is +24.1 mV. The positive value might be due to the presence of one basic nitrogen atom on the surface of NPs. The entrapment efficiency (EE%) value is approximately similar in both NPs.

3.5. Surface morphology

The scanning electron microscopy results of the optimized formulation show an average particle size in the range below 200 nm. The results of the TEM and AFM studies also confirmed the particle size range below 200 nm of the optimized formulation. The prepared nanoparticles are spherical and symmetric, as shown below in Figure 6.

3.6. Differential scanning calorimetry (DSC)

It is an important study to identify the possible interactions between nanoformulation components, *i.e.* a drug and polymer compatibility study. The thermal analysis of the pure drug alendronate showed a sharp peak at 234 °C, indicating its sharp crystalline nature. This temperature corresponds to its melting point. This peak of drug was absent in the NP formulation, which indicates that the drug was encapsulated into the NPs and decreased the crystallinity, which is helpful in drug dissolution. The compatibility study of drug and excipients was identified by DSC and shows that the drug and excipients are compatible with each other and can be used for further formulation development.

3.7. Drug release kinetic study

Drug release is the process in which a drug leaves a drug product and is subjected to ADME, finally becoming available for pharmacological movement. In the *in-vitro* drug release study, the dialysis bag approach was used for nanoparticles, and some mathematical kinetic models, were accomplished. For the kinetic examination of the formulated drug NPs, the plots were made for the zero-order kinetic model, the first-order kinetic model, the Higuchi model, and the Korsmeyer-Peppas model. Plots of the models noted above are shown in Figure 7, and the effects are summarized in Table 2. In the graph, R^2 is the correlation value, k is the rate constant, and n is the release exponent. Based on the above results, the maximum value of R^2 is 0.9685 for the Higuchi model. Therefore, the release study of drug-loaded NPs is followed by the Higuchi model.

Table 2. R^2 values and rate constant values (k) for mathematical models.

Kinetic models	Correlation value (R^2)	Rate constant (k)	Release exponent (n)
Higuchi model	0.9685	0.891×10^{-1} ($min^{-1/2}$)	-
Korsmeyer-Peppas model	0.9154	1.520×10^{-4} (min^{-1})	0.68
First-order model	0.6238	1.140×10^{-1} (min^{-1})	-
Zero-order model	0.9345	2.341 ($mole\times min^{-1}$)	-

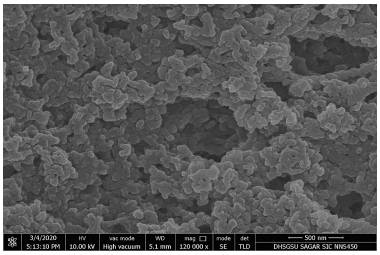
(a)

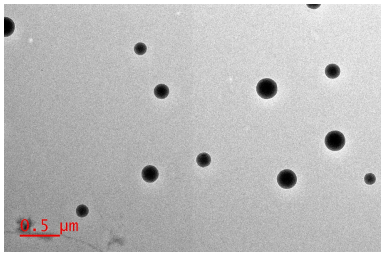

(b)

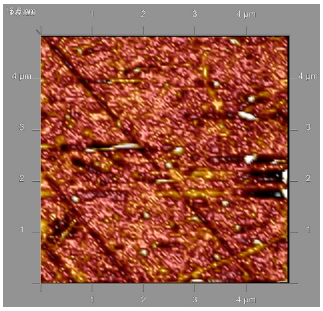
(c)

Figure 6. (a) SEM image of alendronate PLGA NPs, (b) TEM image alendronate PLGA NPs and (c) AFM image of alendronate PLGA NPs.

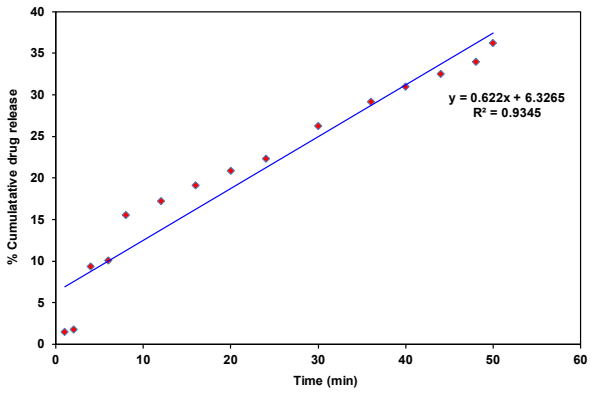

(a)

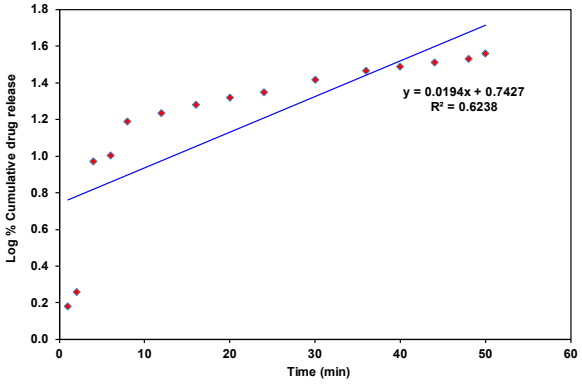

(b)

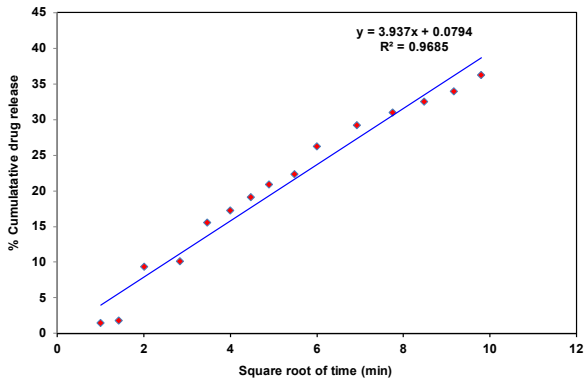

(c)

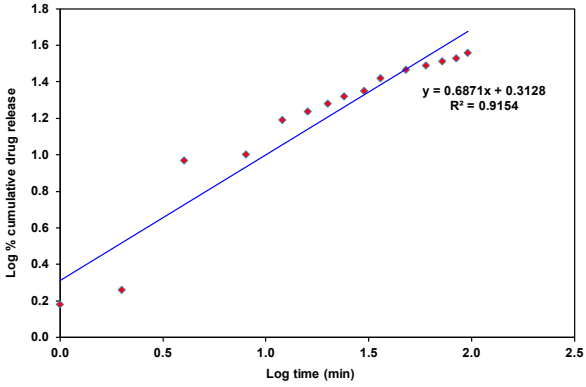

(d)

Figure 7. (a) Zero order plot, (b) First order plot, (c) Higuchi model plot, and (d) Korsemeyer-Peppas model.

In the Korsmeyer-Peppas model, the release exponent value n is 0.68. The magnitude is in the range ($0.45 < n < 0.89$), which indicates that the release mechanism is non-Fickian diffusion.

4. Conclusions

Osteoporosis is the second most severe disease in the current scenario and causes a million fractures per year in the world. Alendronate is the most effective bisphosphonate for the treatment of osteoporosis; in the present work, a novel alendronate-loaded PLGA nanoformulation is proposed for the efficient drug delivery system for the effective management of osteoporosis disease. The effect of different process variables on the preparation of NP was investigated and the *in-vitro* release indicated a controlled and sustained release profile of alendronate-loaded polymeric NP in phosphate buffer saline (pH = 6.8). The release kinetics data showed the highest regression value (R^2) of 0.9685 for the Higuchi model and the '*n*' value (0.68) in the Korsmeyer-Peppas model, indicating that the release mechanism is non-Fickian diffusion. The current study results would help us find a new drug discovery and delivery approach by preparing the anti-osteoporosis drug alendronate in the nano range.

Acknowledgement

The authors are grateful to Electron Microscope Unit AIIMS, New Delhi and IISER (Bhopal) for DLS and DSC studies. We acknowledge Sophisticated Instrumentation Center (SIC), Dr. Harisingh Gour Vishwavidyalaya (A Central University), Sagar for providing us the SEM, TEM and AFM facilities.

Disclosure statement

Conflict of interest: The authors declare that they have no conflict of interest.
Sample availability: Samples of drug-loaded NPs are available from the author.
Ethical approval: There is no need of ethical approval in this manuscript.

CRediT authorship contribution statement

Conceptualization: Sandhya Pathak, Archna Pandey; Methodology: Sandhya Pathak; Software: Sandhya Pathak; Validation: Sandhya Pathak, Sandeep Shukla, Satyendra Kumar Tripathi; Formal Analysis: Sandhya Pathak, Bharat Patel; Investigation: Sandhya Pathak; Resources: Sandhya Pathak; Data Curation: Sandhya Pathak; Writing - Original Draft: Sandhya Pathak; Writing-Review and Editing: Sandhya Pathak, Sandeep Shukla, Archna Pandey; Visualization: Sandhya Pathak; Funding acquisition: Sandhya Pathak; Supervision:, Archna Pandey; Sandhya Pathak, Project Administration: Archna Pandey, Sandhya Pathak.

ORCID and Email

Sandhya Pathak
sandhyapathak935@gmail.com
https://orcid.org/0000-0003-2516-8144
Sandeep Shukla
s.shukla3634@gmail.com
https://orcid.org/0000-0001-6060-8251
Bharat Patel
bharatkp94@gmail.com
https://orcid.org/0000-0002-2754-6965
Satyendra Kumar Tripathi
tripathisatyendra829@gmail.com
https://orcid.org/0000-0001-5310-5461
Archna Pandey
prof.archnapandey@gmail.com
https://orcid.org/0000-0001-7974-2522

References

[1]. Rapp, K.; Rothenbacher, D.; Magaziner, J.; Becker, C.; Benzinger, P.; König, H.-H.; Jaensch, A.; Büchele, G. Risk of nursing home admission after femoral fracture compared with stroke, myocardial infarction, and pneumonia. *J. Am. Med. Dir. Assoc.* **2015**, *16*, 715.e7-715.e12.
[2]. Mithal, A.; Bansal, B.; Kyer, C. S.; Ebeling, P. The Asia-pacific regional audit-epidemiology, costs, and burden of osteoporosis in India 2013: A report of international osteoporosis foundation. *Indian J. Endocrinol. Metab.* **2014**, *18*, 449–454.
[3]. Weaver, C. M.; Alexander, D. D.; Boushey, C. J.; Dawson-Hughes, B.; Lappe, J. M.; LeBoff, M. S.; Liu, S.; Looker, A. C.; Wallace, T. C.; Wang, D. D. Calcium plus vitamin D supplementation and risk of fractures: an updated meta-analysis from the National Osteoporosis Foundation. *Osteoporos. Int.* **2016**, *27*, 367–376.
[4]. Akgun, B.; Avci, D. Synthesis and evaluations of bisphosphonate-containing monomers for dental materials. *J. Polym. Sci. A Polym. Chem.* **2012**, *50*, 4854–4863.
[5]. Gu, W.; Wu, C.; Chen, J.; Xiao, Y. Nanotechnology in the targeted drug delivery for bone diseases and bone regeneration. *Int. J. Nanomedicine* **2013**, *8*, 2305–2317.
[6]. Chourasiya, V.; Bohrey, S.; Pandey, A. Hydrochlorothiazide containing PLGA nanoparticles: Design, characterization, in-vitro drug release and release kinetic study. *Polym. Sci. Ser. B* **2015**, *57*, 645–653.
[7]. Ochiuz, L.; Grigoras, C.; Popa, M.; Stoleriu, I.; Munteanu, C.; Timofte, D.; Profire, L.; Grigoras, A. G. Alendronate-loaded modified drug delivery lipid particles intended for improved oral and topical administration. *Molecules* **2016**, *21*, 858.
[8]. Jagadish, B.; Yelchuri, R.; K, B.; Tangi, H.; Maroju, S.; Rao, V. U. Enhanced dissolution and bioavailability of raloxifene hydrochloride by co-grinding with different superdisintegrants. *Chem. Pharm. Bull. (Tokyo)* **2010**, *58*, 293–300.
[9]. Fasinu, P.; Pillay, V.; Ndesendo, V. M. K.; du Toit, L. C.; Choonara, Y. E. Diverse approaches for the enhancement of oral drug bioavailability. *Biopharm. Drug Dispos.* **2011**, *32*, 185–209.
[10]. Pathak, S.; Vyas, S. P.; Pandey, A. Development, characterization and in vitro release kinetic studies of Ibandronate loaded chitosan nanoparticles for effective management of osteoporosis. *Int. J. Appl. Pharm.* **2021**, 120–125.
[11]. Bohrey, S.; Chourasia, V.; Pandey, A. Preparation, optimization by 23 factorial design, characterization and in vitro release kinetics of lorazepam loaded PLGA nanoparticles. *Polymer Science Series A* **2016**, *58*, 975–986.
[12]. Ali, S. W.; Rajendran, S.; Joshi, M. Synthesis and characterization of chitosan and silver loaded chitosan nanoparticles for bioactive polyester. *Carbohydr. Polym.* **2011**, *83*, 438–446.
[13]. Sivakami, M. S.; Gomathi, T.; Venkatesan, J.; Jeong, H.-S.; Kim, S.-K.; Sudha, P. N. Preparation and characterization of nano chitosan for treatment wastewaters. *Int. J. Biol. Macromol.* **2013**, *57*, 204–212.
[14]. Vhora, I.; Patil, S.; Bhatt, P.; Misra, A. Protein– and Peptide–Drug Conjugates. In *Advances in Protein Chemistry and Structural Biology*; Elsevier, 2015; pp. 1–55.
[15]. Jiang, T.; Yu, X.; Carbone, E. J.; Nelson, C.; Kan, H. M.; Lo, K. W.-H. Poly aspartic acid peptide-linked PLGA based nanoscale particles: potential for bone-targeting drug delivery applications. *Int. J. Pharm.* **2014**, *475*, 547–557.
[16]. Fu, Y.-C.; Fu, T.-F.; Wang, H.-J.; Lin, C.-W.; Lee, G.-H.; Wu, S.-C.; Wang, C.-K. Aspartic acid-based modified PLGA-PEG nanoparticles for bone targeting: in vitro and in vivo evaluation. *Acta Biomater.* **2014**, *10*, 4583–4596.
[17]. Daroszewska, A. Prevention and treatment of osteoporosis in women: an update. *Obstet. Gynaecol. Reprod. Med.* **2012**, *22*, 162–169.
[18]. Miladi, K.; Sfar, S.; Fessi, H.; Elaissari, A. Enhancement of alendronate encapsulation in chitosan nanoparticles. *J. Drug Deliv. Sci. Technol.* **2015**, *30*, 391–396.
[19]. Sastri, K. T.; Radha, G. V.; Pidikiti, S.; Vajjhala, P. Solid lipid nanoparticles: Preparation techniques, their characterization, and an update on recent studies. *J. Appl. Pharm. Sci.* **2020**, *10*, 126–141.
[20]. Rumian, Ł.; Wolf-Brandstetter, C.; Rößler, S.; Reczyńska, K.; Tiainen, H.; Haugen, H. J.; Scharnweber, D.; Pamuła, E. Sodium alendronate loaded poly(l-lactide- co-glycolide) microparticles immobilized on ceramic scaffolds for local treatment of bone defects. *Regen. Biomater.* **2020**, *7*, 293–302.
[21]. Beloqui, A.; Solinís, M. Á.; Rodríguez-Gascón, A.; Almeida, A. J.; Préat, V. Nanostructured lipid carriers: Promising drug delivery systems for future clinics. *Nanomedicine* **2016**, *12*, 143–161.
[22]. Cenni, E.; Granchi, D.; Avnet, S.; Fotia, C.; Salerno, M.; Micieli, D.; Sarpietro, M. G.; Pignatello, R.; Castelli, F.; Baldini, N. Biocompatibility of poly(D,L-lactide-co-glycolide) nanoparticles conjugated with alendronate. *Biomaterials* **2008**, *29*, 1400–1411.
[23]. Vijaykumar, N.; Rueda, J. Nanoparticles for improved delivery of poorly soluble drugs. *J. Drug* **2016**, *1*, 18–27.
[24]. Saini, D.; Fazil, M.; Ali, M. M.; Baboota, S.; Ali, J. Formulation, development and optimization of raloxifene-loaded chitosan nanoparticles for treatment of osteoporosis. *Drug Deliv.* **2015**, *22*, 823–836.
[25]. Cohen-Sela, E.; Chorny, M.; Koroukhov, N.; Danenberg, H. D.; Golomb, G. A new double emulsion solvent diffusion technique for encapsulating hydrophilic molecules in PLGA nanoparticles. *J. Control. Release* **2009**, *133*, 90–95.
[26]. Cohen-Sela, E.; Rosenzweig, O.; Gao, J.; Epstein, H.; Gati, I.; Reich, R.; Danenberg, H. D.; Golomb, G. Alendronate-loaded nanoparticles deplete monocytes and attenuate restenosis. *J. Control. Release* **2006**, *113*, 23–30.

[27]. Pandita, D.; Kumar, S.; Poonia, N.; Lather, V. Solid lipid nanoparticles enhance oral bioavailability of resveratrol, a natural polyphenol. *Food Res. Int.* **2014**, *62*, 1165–1174.
[28]. Dubey, S.; Vyas, S. P. Emulsomes for lipophilic anticancer drug delivery: Development, optimization and in vitro drug release kinetic study. *Int. J. Appl. Pharm.* **2021**, 114–121.
[29]. Bohrey, S.; Chourasiya, V.; Pandey, A. Polymeric nanoparticles containing diazepam: preparation, optimization, characterization, in-vitro drug release and release kinetic study. *Nano Converg.* **2016**, *3*, 3.
[30]. Weng, J.; Tong, H. H. Y.; Chow, S. F. In vitro release study of the polymeric drug nanoparticles: Development and validation of a novel method. *Pharmaceutics* **2020**, *12*, 732.
[31]. Oz, U. C.; Küçüktürkmen, B.; Devrim, B.; Saka, O. M.; Bozkir, A. Development and optimization of alendronate sodium loaded PLGA nanoparticles by central composite design. *Macromol. Res.* **2019**, *27*, 857–866.
[32]. Deca, A. G.; Belu, I.; Croitoru, O.; Bubulică, M. V.; Manda, C. V.; Neamtu, J. Formulation and in vitro evaluation of alendronate sodium/PLGA microspheres for applications in bone related disorders. *Curr. Health Sci. J.* **2015**, *41*, 246–250.
[33]. Liu, Y.-F.; Liu, R.; Li, X.-Y.; Song, Z.; Zhao, X.-H. Development of docetaxel and alendronate-loaded chitosan-conjugated polylactide-co-glycolide nanoparticles: *In vitro* characterization in osteosarcoma cells. *Trop. J. Pharm. Res.* **2016**, *15*, 1353–1360.
[34]. Sandhya, P.; Satyendra Kumar, T.; Chandni, P.; Archna, P. Encapsulation of alendronate in chitosan based polymeric nanoparticles for effective management of osteoporosis – development to release kinetic study. *Int. J. Med. Nano Res.* **2022**, *9*, 036.